Proc. Natl. Acad. Sci. USA
Vol. 91, pp. 4029–4033, April 1994
Biochemistry

Structure and function in rhodopsin: Replacement by alanine of cysteine residues 110 and 187, components of a conserved disulfide bond in rhodopsin, affects the light-activated metarhodopsin II state

(signal transduction/protein folding/G protein-coupled receptors/monoclonal antibody/transducin)

FLORENCE F. DAVIDSON, PETER C. LOEWEN†, AND H. GOBIND KHORANA

Departments of Biology and Chemistry, Massachusetts Institute of Technology, 77 Massachusetts Avenue, Cambridge, MA 02139

Contributed by H. Gobind Khorana, December 1, 1993

ABSTRACT **A disulfide bond that is evidently conserved in the guanine nucleotide-binding protein-coupled receptors is present in rhodopsin between Cys-110 and Cys-187. We have replaced these two cysteine residues by alanine residues and now report on the properties of the resulting rhodopsin mutants. The mutant protein C110A/C187A expressed in COS cells resembles wild-type rhodopsin in the ground state. It folds correctly to bind 11-*cis*-retinal and form the characteristic rhodopsin chromophore. It is inert to hydroxylamine in the dark, and its stability to dark thermal decay is reduced, relative to that of the wild type, by a $\Delta\Delta G^{\ddagger}$ of only −2.9 kcal/mol. Further, the affinities of the mutant and wild-type rhodopsins to the anti-rhodopsin antibody rho4D2 are similar, both in the dark and in light. However, the metarhodopsin II (MII) and MIII photointermediates of the mutant are less stable than those formed by the wild-type rhodopsin. Although the initial rates of transducin activation are the same for both mutant and wild-type MII intermediates at 4°C, at 15°C the MII photointermediate in the mutant decays more than 20 times faster than in wild type. We conclude that the disulfide bond between Cys-110 and Cys-187 is a key component in determining the stability of the MII structure and its coupling to transducin activation.**

Rhodopsin, the vertebrate dim light photoreceptor, is a member of the superfamily of guanine nucleotide-binding protein (G-protein)-coupled signal-transducing membrane proteins. One structural feature in rhodopsin, which is conserved in this class of receptors, is an intradiscal disulfide bond between Cys-110 and Cys-187 (1–5) (Fig. 1). Replacement of either of these cysteine residues in rhodopsin by serine prevents functional receptor formation (4). Likewise, rhodopsin mutants with a short deletion in the N-terminal sequence or in any one of the intradiscal§ loops BC, DE, or FG (Fig. 1) yield completely or partially nonfunctional opsins, as do many point mutants in this domain (6). It has therefore been concluded that the intradiscal loops and the N-terminal region form an integrated tertiary structure, of which the Cys-110 to Cys-187 disulfide bond is a critical component. In the present work¶ we have asked, is rhodopsin able to fold and function correctly when the cysteine residues forming the disulfide bond are replaced by certain amino acids other than serine? Studies of small soluble proteins, such as bovine pancreatic trypsin inhibitor (11–13) and lysozyme (14), have shown that alanine and valine replacements of the disulfide-bonded cysteine residues in these proteins allow the formation of structures virtually identical to those of the native proteins. Moreover, in the β-adrenergic receptor, a member of the G protein-coupled receptor superfamily, valine replacement of the conserved extracellular cysteine pair yields receptors with some ligand-binding capacity (15).

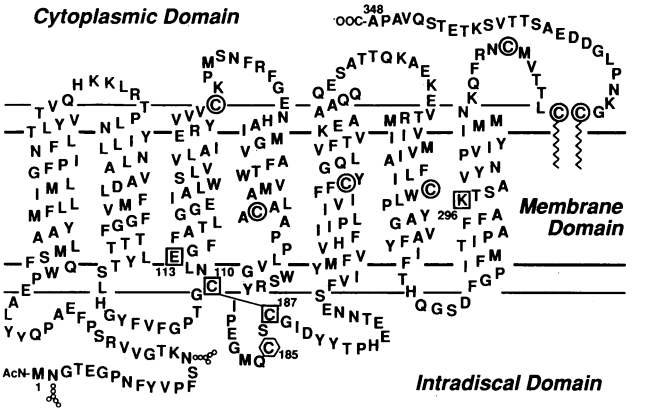

FIG. 1. A secondary structure model for bovine rhodopsin. Shown are (*i*) K296, which forms a Schiff base with 11-*cis*-retinal; (*ii*) E113, counterion to the protonated Schiff base; (*iii*) the 10 cysteine residues of rhodopsin, of which two, C322 and C323, are palmitoylated and two, C110 and C187, form a disulfide bond with each other; and (*iv*) glycosylation sites, N2 and N15. The membrane interface boundaries indicated by double lines are tentative. The intradiscal domain is equivalent to the extracellular domain of related G-protein coupled receptors.

We report here a study of mutant rhodopsins in which one or more of the three intradiscal cysteine residues, 110, 185, or 187 (Fig. 1), has been replaced by alanine. The mutant opsins, expressed in COS-1 cells, fold stably and bind 11-*cis*-retinal to form chromophores with the characteristics of wild-type rhodopsin. By the present criteria, the mutant C110A/C187A has a ground-state structure that is indistinguishable from wild-type rhodopsin, and thermal bleaching shows only a 10% decrease in the transition free energy. However, the metarhodopsin II (MII) intermediate formed by the light-activated mutant is destabilized. At 4°C, under conditions where MII decay is insignificant, initial rates of transducin (G_T) activation by the mutant and wild-type rhodopsins are identical. Yet at 15°C, the decay of mutant MII is at least 20 times faster than that of wild type. Thus, the disulfide bond between Cys-110 and Cys-187 appears to be a key determinant of stability of the MII conformation and its coupling to G_T activation.

The publication costs of this article were defrayed in part by page charge payment. This article must therefore be hereby marked "*advertisement*" in accordance with 18 U.S.C. §1734 solely to indicate this fact.

Abbreviations: G protein, guanine nucleotide-binding protein; G_T, transducin; GTP[γ-^{35}S], guanosine 5′-[γ-[^{35}S]thio]triphosphate; MII, metarhodopsin II; LM, lauryl maltoside.

†Present address: Department of Microbiology, University of Manitoba, Winnipeg, Manitoba R3T 2N2 Canada.

§Usually designated extracellular in other G-protein coupled receptors.

¶This is paper 6 in the series "Structure and Function in Rhodopsin." Paper 5 is ref. 10.

MATERIALS AND METHODS

Expression, Purification, and Characterization of Wild-Type and Mutant Rhodopsins. Mutations in the coding sequence of the synthetic bovine rhodopsin gene (16) were made by cassette mutagenesis as described (17) using the vector pMT4 (18). COS-1 cells were transiently transfected with mutant and wild-type plasmids (17), harvested 60–72 h later, and resuspended in PBS buffer (1.5 mM KH_2PO_4/8 mM Na_2HPO_4/2.7 mM KCl/137 mM NaCl, pH 7.3) containing benzamidine, aprotinin, leupeptin, and pepstatin A each at 25 μg/ml and phenylmethylsulfonyl fluoride at 0.1 mM. Expressed opsins were reconstituted by the addition of 11-*cis*-retinal (5 μM) to the cell suspension, followed by gentle agitation for 2 h at 4°C in the dark. Reconstituted rhodopsins were solubilized with 1% (wt/vol) lauryl maltoside (LM; Anatrace, Maumee, OH), incubated for 2 h at 4°C in the dark, and centrifuged for 1 h at 100,000 × *g* at 4°C. Rhodopsins were purified from the 100,000 × *g* supernates by immunoaffinity chromatography using rho1D4-Sepharose (17) in 0.05% LM in 10 mM sodium phosphate buffer (pH 6.0) or 50 mM Tris·HCl, pH 7.0/150 mM NaCl. Purity of the immunopurified rhodopsins was assessed after SDS/PAGE in 10–12% polyacrylamide gels (19) by silver staining (Bio-Rad silver stain plus kit), by immunoreactivity against the monoclonal antibody rho1D4, and by measurement of the absorbance ratios at 280 nm to 500 nm (A_{280}/A_{500}) in the UV–visible spectrum (20).

UV–Visible Spectroscopy. All measurements were made on a Perkin–Elmer λ7 UV–visible spectrometer, equipped with water-jacketed cuvette holders connected to a circulating water bath (model RTE 5DD, Neslab Instruments, Portsmouth, NH). Temperatures at the cuvette were monitored by a digital thermometer mounted on the sample cuvette holder (Cole–Parmer model 8402-00). Samples were illuminated in the cuvettes with a 150-W fiber optic light (Dolan–Jenner, Woburn, MA; Fiber Lite A-200) equipped with a 495-nm cutoff filter (Melles Griot, Irvine, CA). The absorbance due to any remaining ground-state mutant or wild-type rhodopsin was determined at the end of each experiment by inertness to added 100 mM hydroxylamine and was subtracted from all spectra shown. This amounted to <15% of the total initial chromophore in all cases.

Measurement of Extinction Coefficients. Relative extinction coefficients of mutant and wild-type rhodopsins were measured using acid denaturation (21). Absorption spectra of samples were taken in the dark at 15°C, and an aliquot of 1 M H_2SO_4 was added to a final concentration of 0.01 M (pH 1.5–2.0). The ratio of the resulting absorbance at 440 nm (due to protonated retinyl Schiff base) to the initial absorbance at 500 nm was then computed and used to determine the relative extinction coefficients of wild-type and mutant rhodopsins.

ELISA. The relative affinities of the wild-type and mutant rhodopsins for the monoclonal antibody rho4D2 were measured using competition ELISAs as described (22), except that serial dilutions of the rhodopsins were made in PBS buffer containing 0.05% LM. Aliquots of each dilution were added to equal volumes of rho4D2 hybridoma supernates and incubated in the dark, or in room light after a 2-min illumination with >495-nm light, for 30 min at 4°C. Aliquots of the binding reactions were then added to microtiter plate wells coated with immobilized rod outer segment rhodopsin, and the mixtures were incubated 30 min at 4°C. Unbound proteins were then washed away, and peroxidase-conjugated sheep anti-mouse IgG (Amersham) was added for 30 min. Excess peroxidase-conjugated IgG was washed away before adding 2,2′-azinobis(3-ethylbenzthiazoline)-6-sulfonic acid, the peroxidase substrate. Reactions were monitored using a Bio-Tek (Burlington, VT) automated ELISA reader equipped with a 405-nm filter.

Determination of Thermal Stabilities. The thermal stability of ground-state rhodopsins was measured by monitoring the rate of loss of 500-nm absorbance and appearance of 380-nm absorbance as a function of temperature in the dark. At temperatures where decay of the chromophore was slow, measurements were made by repetitive scanning at 240 nm/min from 650 nm to 250 nm. At higher temperatures, scans were taken before and after the experiment, to look for any changes in baseline, light scattering, or loss of sample, and the decay kinetics were monitored by single-wavelength measurements at 510 nm. The decays were fit to single exponentials using the KALEIDAGRAPH program (Synergy Software, Reading, PA). From these, the first-order decay rate constants were derived. The thermodynamic parameters E_a, $\Delta G^{\ddagger}$, $\Delta H^{\ddagger}$, and $\Delta S^{\ddagger}$ were calculated from the rate data according to standard theory for irreversible processes (23) using values for the slopes of the Arrhenius plots which were derived from least-squares analysis.

Assay for G_T Activation. G_T activation was measured by the light-stimulated formation of the $G_{T\alpha}$–guanosine 5′-[γ-[^{35}S]thio]triphosphate (GTP[γ-^{35}S]) complex, as described (24) with the following modifications. Assays were carried out using 1–12.5 nM rhodopsin, as indicated, 250 nM G_T (25), and 125 nM GTP[γ-^{35}S] (1.4 × 10^5 cpm/pmol) in 10 mM Tris·HCl, pH 7.4/100 mM NaCl/0.5 mM $MgCl_2$/1 mM dithiothreitol/0.0125% LM. Reactions were initiated by the addition of GTP[γ-^{35}S] to rhodopsin/G_T mixes preequilibrated at 4°C in the dark, with and without prior illumination for 90 sec with >495-nm light. Four 25-μl aliquots were removed at 15- to 30-sec intervals and filtered through nitrocellulose (Millipore HAWP-45 μm). The filters were rinsed three times with ice-cold buffer, dried, and subjected to scintillation counting to quantitate bound $G_{T\alpha}$–GTP[γ-^{35}S]. Dark activities were subtracted from light activities for each time point, and the data were analyzed by linear regression to determine the rates of rhodopsin-catalyzed exchange of GTP[γ-^{35}S] for GDP. Dark activities were <1% of the light-activated signal. Non-initial-rate assays were performed under exactly the same conditions, but binding was assessed only after a 6-h incubation. Values reported for both types of assays are the results of duplicate or triplicate experiments.

RESULTS

Mutants Lacking a Cys-110 to Cys-187 Disulfide Bond Form Native-Like Dark-State Rhodopsin. Rhodopsin mutant genes containing the substitutions C187A, C110A/C187A, and C110A/C185A/C187A were transiently expressed in COS-1 cells, and the resulting opsins were reconstituted with 11-*cis*-retinal and purified. Fig. 2 shows the UV–visible absorption spectra of the wild-type and the mutant rhodopsins. All three mutants showed spectra characteristic of the wild-type

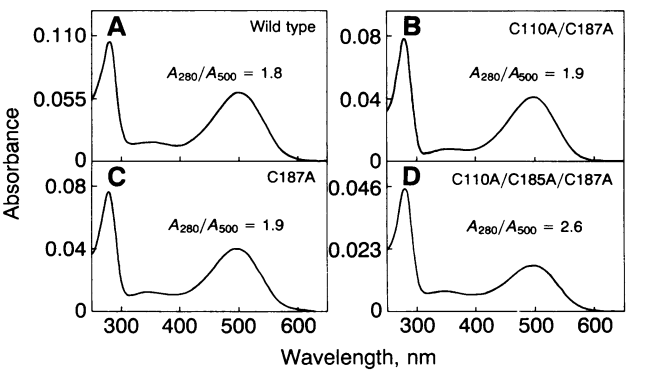

FIG. 2. UV–visible absorption spectra of wild-type and mutant rhodopsins, after expression of the corresponding opsin genes in COS-1 cells and immunopurification.

rhodopsin, with visible absorption maxima at 498 ± 2 nm. Overlays of the spectra (not shown) verified that the bandwidths were similar, although all three mutants showed a slight (3–4 nm) blue shift apparent only at the sides of the visible absorbance peaks. The relative extinction coefficients at 500 nm for C110A/C187A and C187A were equivalent, within experimental error, to that of the wild-type rhodopsin (0.94, 0.94, and 1.00, ± 0.10, respectively). Based on the 500-nm absorbing material recovered, the mutant opsins were obtained at lower yields than the wild-type protein. Typically, the yields relative to wild-type were 50–70% for C110A/C187A and C187A and 20–30% for C110A/C185A/C187A. The A_{280}/A_{500} (Fig. 2) indicated that the C110A/C187A and C187A rhodopsin preparations were at least 80% pure and that the triple mutant C110A/C185A/C187A was about 65% pure, compared to the wild type. Results of SDS/PAGE showed no detectable amount of non-opsin proteins in any of the samples. Tests of the reactivity of the wild-type, C110A/C187A, and C187A Schiff bases to 100 mM hydroxylamine showed that, like wild type, the mutants were inert for at least 1 h at 20°C in the dark and reacted only upon illumination to form the expected 360-nm retinal oxime species (data not shown).

Thermal Stability of the Rhodopsin Mutant C110A/C187A. The double mutant C110A/C187A was used for further characterization. Thermal stabilities of wild-type and C110A/C187A mutant rhodopsin chromophores were determined, in the dark. Rates of thermal decay were measured at selected temperatures by the decrease in absorption at 500 nm (i.e., loss of the opsin shift). Wild-type rhodopsin decay at 55°C in LM is shown in Fig. 3*A*. A similar decay of the mutant C110A/C187A was observed at significantly lower temperatures, such as 41°C (Fig. 3*B*). Fig. 3*C* shows the Arrhenius plot of decay rate constants vs. $1/T$, from which the thermodynamic parameters shown in Table 1 were derived. The slopes of the Arrhenius plots are parallel, within

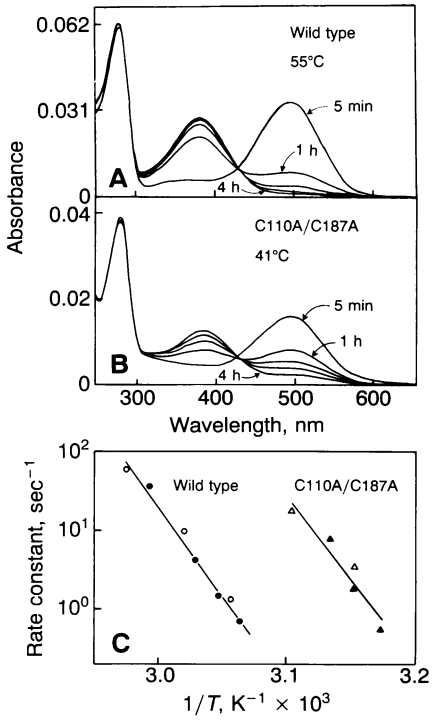

FIG. 3. Measurement of the thermal stabilities of wild-type and mutant rhodopsins in the dark state. (*A* and *B*) Representative spectra are shown for the temperature-dependent loss of 500-nm absorption and the increase at 380 nm. (*A*) Purified wild type. (*B*) C110A/C187A mutant rhodopsin. (*C*) Arrhenius plot of the decay rate constant vs. (temperature)$^{-1}$ for wild-type (●, ○) and C110A/C187A (▲, △) rhodopsins.

Table 1. Thermodynamic parameters for the dark thermal bleaching of wild-type and C110A/C187A mutant rhodopsins

Parameter, kcal/mol	Rhodopsin	
	Wild type	C110A/C187A
E_a	102.1 ± 5.8	97.7 ± 18.6
$\Delta G^{\ddagger}$	25.7 ± 0.6	22.8 ± 0.6
$\Delta\Delta G^{\ddagger}$	—	−2.9 ± 1.2
$\Delta H^{\ddagger}$	101.5 ± 4.9	97.1 ± 18.6

experimental error, for the wild-type and mutant rhodopsins. Therefore, the $\Delta H^{\ddagger}$ values are also the same (Table 1). Comparison of the $\Delta G^{\ddagger}$ for thermal loss of chromophore in C110A/C187A to that in the wild-type COS cell-expressed rhodopsin gave a $\Delta\Delta G^{\ddagger}$ value of −2.9 ± 1.2 kcal/mol.

The Photoproduct MII of C110A/C187A Mutant Rhodopsin Is Less Stable Than That of Wild-Type Rhodopsin. Spectral changes observed in the mutant and wild-type rhodopsins in response to light are shown in Fig. 4. Wild-type rhodopsin in LM (Fig. 4*A*) probed 15 sec after saturating illumination (spectrum 2) showed predominantly the MII photoproduct (λ_{max} = 384 nm), as expected. Repetitive subsequent scanning showed that this species decayed to a mixture of species. Free all-*trans*-retinal was formed, as evidenced by the shift of the absorption maximum from 384 nm to 388 nm and, separately, by following absorption at 360 nm after acidification. The MIII intermediate (λ_{max} = 465 nm) was also

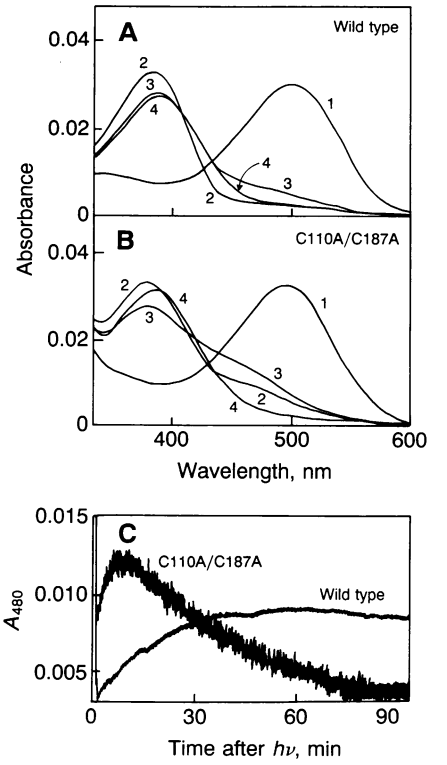

FIG. 4. Changes in the absorption spectra of wild-type and C110A/C187A mutant rhodopsins after illumination in LM. UV–visible absorbance spectra of the wild-type (*A*) and mutant (*B*) rhodopsin were recorded at 15°C in the dark (curves 1) and after illumination for 15 sec using >495-nm light (curves 2–4). Scans were taken starting immediately after illumination (curves 2) and at intervals of 2.5 min thereafter. The scans shown as curves 3 were taken after 60 min (*A*) or 5 min (*B*), when apparent MIII accumulation was maximum; curves 4 were taken after 9 h (*A*) or 2.75 h (*B*), when the formation of free all-*trans*-retinal was judged to be complete. (*C*) Rise and decay of MIII, monitored by absorbance at 480 nm. All the absorbances are normalized to the same initial absorbances at 500 nm before photoconversion.

formed, as seen by difference spectroscopy (spectrum 3 minus spectrum 4) and reached a maximum in about 60 min (spectrum 3). In about 9 h, the MIII signal decayed completely to free retinal and opsin (spectrum 4).

Fig. 4*B* shows the bleaching behavior of the mutant C110A/C187A rhodopsin under the same conditions. In contrast to wild type, saturating illumination produced a mixture of species within 15 sec (spectrum 2). The initial absorbance at 384 nm was lower than that observed for wild type, and there was also significant absorption at longer wavelengths. The absorption in the latter region increased for up to 5 min (spectrum 3), and difference spectra (e.g., spectrum 3 minus spectrum 4) revealed, as in the wild type, the formation of a 465-nm absorbing peak characteristic of the MIII intermediate. The absorption at 465 nm reached a maximum in 5 min, and its amplitude was twice that observed in wild type in 60 min (see above). The formation and decay of the MIII intermediate in the mutant relative to wild type was also compared by monitoring absorption changes at 480 nm (Fig. 4*C*). These data further demonstrated that the formation of MIII in the mutant was at least 20-fold faster and its decay at least 6 times faster than those in the wild type. The mutant decayed fully to free retinal and opsin in less than 2.8 h (Fig. 4*B*, spectrum 4). Qualitatively similar results were obtained at 4°C for photobleaching of both wild type and the mutant.

Light-Dependent Activation of G_T by the C110A/C187A Mutant Rhodopsin. C110A/C187A rhodopsin activated G_T, as assayed by the light-stimulated exchange of GTP[γ-^{35}S] for $G_{T\alpha}$-bound GDP. As seen in Fig. 5*A*, the initial rates of activation by the mutant and wild-type COS cell rhodopsins, as well as that of native rod outer segment rhodopsin, were identical at 4°C in the rhodopsin concentration range of 1–10 nM. The initial rates were derived from time courses displaying burst kinetics, and the amplitudes of the bursts, due to preformed R^*–G_T complexes, were identical for wild type and mutant (data not shown). Selwyn's plots (24) of the rate data indicated no change in R^* concentrations during the initial rate assays for either wild type or mutant (data not shown).

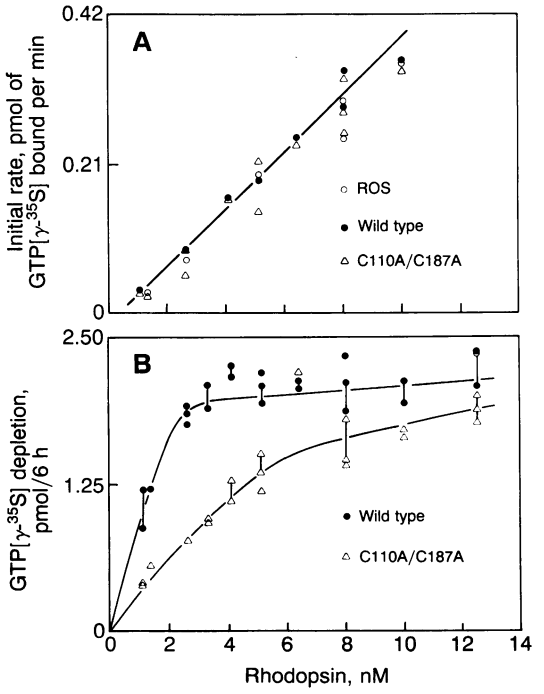

FIG. 5. GDP–GTP[γ-^{35}S] exchange assay of G_T activation by wild-type and mutant rhodopsins. (*A*) Initial rate vs. rhodopsin concentrations at 4°C. (*B*) Assays of total GTP[γ-^{35}S] utilization in 6 h at 4°C. ROS, rod outer segment rhodopsin.

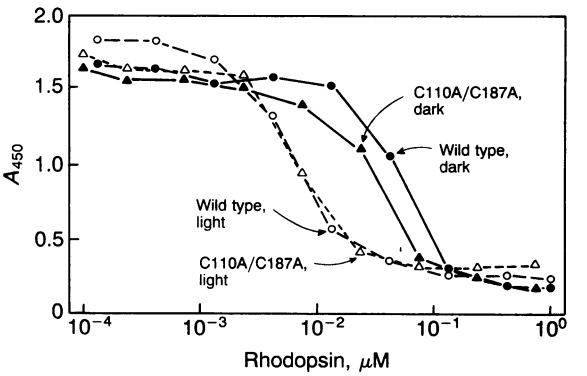

FIG. 6. Relative affinities of the anti-rhodopsin monoclonal antibody rho4D2 for wild-type (●, ○) and C110A/C187A (▲, △) rhodopsins in the dark (●, ▲) and after illumination (○, △) as determined by ELISA.

Assays of G_T activation over long times (Fig. 5*B*) showed differences in GTP[γ-^{35}S] utilization by C110A/C187A compared to wild type. In a 6-h incubation, about 5-fold more C110A/C187A mutant was required to deplete the available GTP[γ-^{35}S] than was needed for the wild type.

Structural Changes in the Mutant and Wild-Type Rhodopsin in Response to Light, as Probed by Immunoreactivity. The monoclonal anti-rhodopsin antibody rho4D2 recognizes the N-terminal amino acid sequence 2–38 and shows about a 10-fold higher affinity for photobleached rhodopsin than for ground-state rhodopsin (ref. 1; L. Molday, personal communication). The binding of the wild-type and C110A/C187A rhodopsins to rho4D2 was tested in LM both in the dark and after illumination. The binding affinities of wild-type and mutant rhodopsins for rho4D2 were similar in the dark and after illumination; there was a 10-fold increase in affinity after illumination (Fig. 6).

DISCUSSION

A highly significant finding of the present work is that a disulfide bond between Cys-110 and Cys-187 is not essential for the correct *in vivo* folding of bovine opsin. By all the present criteria, the tertiary structures of the wild-type and C110A/C187A mutant rhodopsins, formed by reconstitution with 11-*cis*-retinal, are similar in the ground state. Thus, the mutant opsin binds 11-*cis*-retinal to form rhodopsin with chromophore characteristics matching those of native rhodopsin. The environment around the Schiff base in the folded mutant rhodopsin is similar to that in native rhodopsin, as inferred from its inertness to hydroxylamine in the dark. Further, the mutant rhodopsin does not activate G_T in the dark, in contrast with certain other rhodopsin mutants that show constitutive G_T activation (26). Finally, a comparison of the binding affinities to the monoclonal antibody rho4D2 also indicates that the conformations of the intradiscal domain in the mutant and wild-type rhodopsins are similar in the dark and after photoactivation. The slightly higher affinity (<2-fold) of the antibody for the mutant C110A/C187A in the dark may suggest a greater conformational flexibility in the intradiscal domain in the absence of the disulfide bond.

Alanine replacements of cysteine residues 110 and 187 satisfied the structural requirements at these sites for opsin folding and stability. In earlier work, mutants with substitution of serine for cysteine at these positions failed to form functional rhodopsin (4). However, serine is a hydrophilic amino acid and is virtually absent from naturally occurring mutations at buried disulfide-bonded cysteine residues (27). Our present data do not prove that there are no differences between wild-type and C110A/C187A opsins in the ground

state. Indeed, the absence of the covalent disulfide bond and sulfur atoms constitutes a de facto structural change. Also, the slight blue shift reported for the ground-state visible absorbance spectrum suggests that the electronic environment of the retinyl Schiff base may sense either the sulfur of Cys-187 itself or the positioning of Cys-110 or other amino acids in the presence of Cys-187. This effect is not large; however, its magnitude is less than that seen on shortening the Schiff base counterion Glu-113 by one carbon, to an aspartic acid (21).

Equilibrium folding and unfolding studies of small soluble proteins have suggested that disulfide bonds have a global stabilizing effect on the folded state primarily by decreasing the entropy of the unfolded state (e.g., ref. 28). The studies reported here, in fact, suggest that a small destabilization of the retinal binding pocket of rhodopsin occurs upon Cys-110/Cys-187 replacement, without significant changes in the enthalpic contributions to the transition. This suggests no significant loss or rearrangement of weak bonding and nonbonding interactions, such as would accompany a gross defect in packing. Our measurements do not rule out the possibility that there is a small effect on $\Delta H^{\ddagger}$. However, the data are consistent with destabilization arising primarily from an increased $\Delta S^{\ddagger}$ in the mutant rhodopsin.

Light activation of rhodopsin following 11-*cis*- to all-*trans*-retinal isomerization results from conformational changes that occur, on a progressively slower time scale, via thermal relaxation (29). The species MII represents the conformation that activates G_T (7, 30). MII is formed in milliseconds (8); it appears to decay in LM, as in digitonin (9), both directly to opsin and all-*trans*-retinal and to MIII, which then decays to opsin and retinal. The present data (Fig. 4*A*) as well as those of D. Farrens (unpublished results) in this laboratory are consistent with this interpretation. The mutant C110A/C187A on light activation clearly forms the MII intermediate, as shown by the identical rates of activation of G_T at 4°C by the mutant and wild-type rhodopsins. Moreover, the mutant MII appears to have the same affinity for G_T as does wild type, based on the identical bursts in the initial rate assays. However, this intermediate is clearly destabilized in the mutant: the rapid rise and decay of the MIII intermediate in the mutant (Fig. 4) to form opsin and free retinal and the lower efficiency of G_T activation over longer times (Fig. 5*B*) all point to destabilization of MII in the mutant. In an independent study, Garcia-Quintana *et al.* (31) have reported accelerated MIII decay in the native rhodopsin treated with dithiothreitol, which is consistent with the rhodopsin mutant results reported here.

Destabilization of the MII intermediate in the C110A/C187A mutant is thus the most striking consequence of the absence of the two cysteine residues. How do cysteine residues 110 and 187 stabilize the MII conformation without being required for formation of the catalytic structure of the MII–G_T complex? Does absence of the two sulfurs cause a loss of stabilizing electronic interactions in the vicinity of the Schiff base and associated protonation/deprotonation network, or is the destabilization associated with their absence primarily entropic in origin, analogous to the effects observed in the ground state? A conformational change in the intradiscal domain upon photoactivation is indeed indicated for both wild type and mutant (Fig. 6).

In summary, the central conclusion of this study is that cysteine residues 110 and 187 are involved in stabilizing that conformation of the light-activated rhodopsin that is required for signal transduction. The conserved disulfide bond clearly influences the energetics of transmembrane signal transduction. A separate recent study has shown the importance of intradiscal N-linked glycosylation in signal transduction by rhodopsin (10). Thus the results to date show that the propagation of light-activated conformational change, originating in the membrane domain of rhodopsin, involves both the cytoplasmic and the intradiscal domains.

We are grateful to Ms. Laurie Molday and Prof. Robert Molday for instruction in the use and interpretation of the ELISA technique and to Mr. John Rhee for assistance in the construction of mutants. We would also like to express our appreciation to Prof. Paul Schimmel and Peter Kim and Drs. Kevin Ridge, Robin Thurmond, Mark Krebs, Xun Liu, David Farrens, and John Resek for reading the manuscript and to Ms. Judy Carlin for assistance in the preparation of the manuscript. This work was supported by a grant from the National Institutes of Health (GM 28289). F.F.D. was supported by a Damon Runyon–Walter Winchell Cancer Research Fund Fellowship (DRG-1071; 1990–1993).

1. Al-Saleh, S., Gore, M. & Akhtar, M. (1987) *Biochem. J.* **246,** 131–137.
2. Findlay, J. B. C. & Pappin, D. J. C. (1986) *Biochem. J.* **238,** 625–642.
3. Karnik, S. S. & Khorana, H. G. (1990) *J. Biol. Chem.* **265,** 17520–17524.
4. Karnik, S. S., Sakmar, T. P., Chen, H.-B. & Khorana, H. G. (1988) *Proc. Natl. Acad. Sci. USA* **85,** 8459–8463.
5. Probst, W. C., Snyder, L. A., Schuster, D. I., Brosius, J. & Sealfon, S. C. (1992) *DNA Cell Biol.* **11,** 1–20.
6. Doi, T., Molday, R. S. & Khorana, H. G. (1990) *Proc. Natl. Acad. Sci. USA* **87,** 4991–4995.
7. Kibelbek, J., Mitchell, D. C., Beach, J. M. & Litman, B. J. (1991) *Biochemistry* **30,** 6761–6768.
8. Hoffman, K. P. (1993) *Proc. Natl. Acad. Sci. USA* **90,** 7849–7853.
9. Blazynski, C. & Ostroy, S. E. (1984) *Vision Res.* **24,** 459–470.
10. Kaushal, S., Ridge, K. D. & Khorana, H. G. (1994) *Proc. Natl. Acad. Sci. USA* **91,** 4024–4028.
11. Staley, J. S. & Kim, P. (1992) *Proc. Natl. Acad. Sci. USA* **89,** 1519–1523.
12. Marks, C. B., Naderi, H., Kosen, P. A., Kuntz, I. D. & Anderson, S. (1987) *Science* **235,** 1370–1373.
13. Eigenbrot, C., Randal, M. & Kossiakoff, A. A. (1992) *Proteins Struct. Funct. Genet.* **14,** 75–82.
14. Inaka, K., Taniyama, Y., Kikuchi, M., Morikawa, K. & Matsushima, M. (1991) *J. Biol. Chem.* **266,** 12599–12603.
15. Dixon, R. A. F., Sigal, I. S., Candelore, M. R., Register, R. B., Scattergood, W., Rands, E. & Strader, C. D. (1987) *EMBO J.* **6,** 3269–3275.
16. Ferretti, L., Karnik, S. S., Khorana, H. G., Nassal, M. & Oprian, D. D. (1986) *Proc. Natl. Acad. Sci. USA* **83,** 599–603.
17. Oprian, D. D., Molday, R. S., Kaufman, R. J. & Khorana, H. G. (1987) *Proc. Natl. Acad. Sci. USA* **84,** 8874–8878.
18. Franke, R. R., Sakmar, T. P., Oprian, D. D. & Khorana, H. G. (1988) *J. Biol. Chem.* **263,** 2119–2122.
19. Laemmli, U. K. (1970) *Nature (London)* **227,** 680–685.
20. Hargrave, P. A. (1982) in *Progress in Retinal Research*, eds. Osbourne, N. N. & Chader, G. S. (Pergamon, Oxford, U.K.), pp. 1–51.
21. Sakmar, T. P., Franke, R. R. & Khorana, H. G. (1989) *Proc. Natl. Acad. Sci. USA* **86,** 8309–8313.
22. Laird, D. W., Wong, S. Y. C. & Molday, R. S. (1987) in *Membrane Proteins: Proceedings of the Membrane Protein Symposium*, ed. Goheen, S. C. (Bio-Rad Lab., Richmond, CA), pp. 45–70.
23. Segel, I. H. (1975) *Enzyme Kinetics* (Wiley, New York), pp. 931–941.
24. Wessling-Resnick, M. & Johnson, G. L. (1987) *J. Biol. Chem.* **262,** 3697–3705.
25. Fung, B. K. K., Hurley, J. B. & Stryer, L. (1981) *Proc. Natl. Acad. Sci. USA* **78,** 152–156.
26. Robinson, P. R., Cohen, G. B., Zhukovsky, E. A. & Oprian, D. D. (1992) *Neuron* **9,** 719–725.
27. Overington, J., Donnelly, D., Johnson, M. S., Sali, A. & Blundell, T. L. (1992) *Protein Sci.* **1,** 216–226.
28. Shortle, D. (1992) *Q. Rev. Biophys.* **25,** 205–250.
29. Birge, R. R. (1990) *Biochim. Biophys. Acta* **1016,** 293–327.
30. Bennet, N., Michel-Villaz, M. & Kuhn, H. (1982) *Eur. J. Biochem.* **127,** 97–103.
31. Garcia-Quintana, D., Garriga, P., Dunach, M. & Manyosa, J. (1992) *Struct. Funct. Retinal Proteins* **221,** 295–298.